ELSEVIER

Journal of Pharmaceutical and Biomedical Analysis
28 (2002) 269–278

JOURNAL OF
PHARMACEUTICAL
AND BIOMEDICAL
ANALYSIS

www.elsevier.com/locate/jpba

An equivalent length model of microdialysis sampling

Sheng Tong, Fan Yuan *

Department of Biomedical Engineering, Box 90281, Duke University, Durham, NC 27708, USA

Received 18 April 2001; received in revised form 14 September 2001; accepted 26 September 2001

Abstract

One of the critical issues in microdialysis sampling is how to predict the extraction fraction (E_d), based on transport properties of analytes in both tissues and probes. A one-dimensional (1-D) model has been used widely in previous studies to predict E_d at the steady state. However, this model is valid only for long probes. To this end, an equivalent length (EL) model was developed for probes with any length used in experiments. The key idea in the model was to replace the probe length (L) in the 1-D model with an equivalent length (L_E) when calculating transport resistance in surrounding tissues. The length difference, ($L_E - L$), was assumed to be proportional to the penetration depth of analytes (Γ). The proportionality constant (λ) was determined through minimizing the errors in predicted E_d. We found that, the EL model could accurately predict E_d when $\lambda = 0.369$. The maximum error in EL model predictions was $< 6\%$, for model constants varying in the same ranges as those in microdialysis experiments. This error was one order of magnitude smaller than that in 1-D model predictions.

Keywords: Microdialysis; Extraction fraction; Drug delivery

1. Introduction

Microdialysis is currently one of a few techniques that can be used to monitor drug delivery in patients [1]. The technique has several advantages [2–6]. First, it can be well tolerated by patients, although, it is invasive. Second, microdialysis sampling does not require anesthesia once the probe is implanted. Thus, it allows a direct, long term and repeated sampling of interstitial concentration of drugs as well as local chemical environment in tissues. The temporal resolution of sampling can be as short as a minute. Third, it does not require labeling of drugs with specific markers, in contrast to other in vivo techniques (e.g. magnetic resonance imaging (MRI) and positron emission tomography (PET)). Fourth, samples can be collected both before and after treatment. Thus, each individual patient can serve as his/her own control. This advantage reduces the number of patients in experiments and effects of patient-to-patient variations on experimental results. Fifth, drug metabolism in tissues can be studied locally, without systemic involvement, through direct infusion of drugs via a microdialysis probe and collection of metabolites using the same probe. Sixth, it samples free drug instead of total drug in tissues. The former is more directly

* Corresponding author. Tel.: +1-919-660-5411; fax: +1-919-684-4488.
E-mail address: fyuan@acpub.duke.edu (F. Yuan).

0731-7085/02/$ - see front matter
PII: S0731-7085(01)00565-9

correlated with the efficacy of drugs. Finally, the sampling procedure excludes macromolecules in the interstitial space, and thus enzymatic degradation and/or inactivation of drugs during the sample processing are eliminated. These advantages make microdialysis an important sampling technique in several research fields, including pharmacokinetics and metabolism of drugs in various organs [2–6], chemical microenvironment in tissues, and cytokines involvement in tissue damage and wound healing [7–9].

Microdialysis sampling is performed at non-equilibrium states. The concentration of analytes in the dialysate (C_{out}) is always lower than, although, can be close to, that in the interstitial space prior to probe implantation (C_∞). The ratio of the concentrations (i.e. C_{out}/C_∞) is defined as the recovery, E_d. When the concentration of the analytes in the perfusate (C_{in}) is comparable with C_{out} a more general definition of E_d is $(C_{out} - C_{in})/(C_\infty - C_{in})$, which is also called extraction fraction in the literature [10]. E_d depends on transport properties of analytes in the probe and tissues, as well as the perfusion rate of dialysate. Once E_d is determined for a specific combination of probes and tissues, the absolute concentration of drugs in the interstitial space can be calculated from experimental data of C_{in} and C_{out}.

One of the key issues in microdialysis sampling is, how to determine E_d through probe calibration. Probe calibration is tissue- and drug-dependent, since transport of drugs from the surrounding tissues into the probe is a diffusion process, which depends on molecular properties of drugs, as well as structures of the probe and tissues. In addition, C_∞ is unknown in most applications, and may vary with time due to metabolism of drugs. Thus, in vivo calibration of microdialysis sampling is complicated [6].

To better understand how different factors affect in vivo calibration and microdialysis sampling, various mathematical models have been developed [11]. Most of them are based on empirical curve fitting of experimental data. These models are experimentally useful in calibrating microdialysis probes, but cannot predict E_d in terms of probe geometry and transport parameters. Other models, referred to as explicit models in the literature (for review see [6,11]), are capable of predicting E_d based on the theory of molecular transport. General explicit models of microdialysis can be easily developed, but it is difficult to obtain analytical solutions when both transport and metabolism of analytes are considered in a three-dimensional (3-D) space and in a time-dependent manner. Therefore, explicit models in previous studies had to either, neglect transport across the microvessel wall and metabolism of drugs in tissues [12], or assume that the transport of analytes from tissues to the probe was one-dimensional (l-D) and in the direction perpendicular to the probe [10,13,14]. Most studies prefer the l-D assumption, since transvascular transport and metabolism of drugs are critical and cannot be neglected in pharmacokinetic analyses. A popular l-D model for the steady state sampling was developed by Bungay et al., [10]. To simplify the discussion, we named the model as BMD after the first letters of three co-authors. The BMD model provides a set of analytical equations that can predict E_d as a function of probe geometry and transport parameters in tissues and the probe [10]. However, an important question remains to be answered: what are the limitations of the 1-D assumption?

The goal of the present study is 2-fold, (i) to estimate the error in the predicted E_d caused by the 1-D assumption at the steady state; and (ii) to develop an EL theory to minimize the error. The error analysis of E_d was performed through comparisons of model predictions between the BMD and a two-dimensional (2-D) model. The 2-D model was similar to the BMD model, except that diffusion in the direction of perfusion was considered as well. Based on the error analysis, an EL theory was developed. The key idea in the new model was to use an EL to replace the probe length in the BMD model so that the same analytical equations can be used to predict E_d. As a result, the maximum error in EL model predictions was $< 6\%$, which was one order of magnitude smaller than that in BMD model predictions.

2. Methods

Probe design depends on biological applications. Probes used in previous studies can be, in general, divided into three categories, (i) cannula-style; (ii) linear; and (iii) flow-through [5]. The length of probes may vary from 1 mm to several centimeters. The present study was focused on the cannula-style probes, since they have been widely used in pharmacokinetic studies. The key assumptions in the present study were, (a) the volume fraction of interstitial fluid near the probe was uniform and would not change during microdialysis sampling; and (b) concentration distribution of analytes was axisymmetric about the central axis of the probe and at the steady state.

2.1. The 2-D mathematical model

2.1.1. Model geometry

The exchange of the analytes between the probe and surrounding tissues was determined by its transport in three continuous regions: the annulus, the semipermeable membrane, and the tissues (Fig. 1). These regions are concentric about the central axis of the probe. Thus, the cylindrical coordinate system was used in the study. Initially, the concentration of analytes was uniform throughout the entire tissue. Microdialysis sampling caused a reduction in the concentration in the region around the probe. The radius of the region, Π, depended on transport parameters and the length of the probe. We found in a preliminary study that Π was <6 mm for the ranges of model constants used in this study. Thus, the region of the simulation was chosen to be a cylinder with the radius of 6 mm $+ r_0$, and the height of 12 mm $+ L$, where r_0 and L were the outer radius and the length of the probe, respectively (Fig. 1).

2.1.2. Transport in the annulus

The transport of analytes in the annulus involves both convection and diffusion. By carefully controlling hydrostatic and osmotic pressures, one can exclude convection across the probe membrane so that diffusion is the only mode of transport across the membrane and convection occurs only in the probe due to the perfusion. The present study assumed that the convection of the dialysate in the probe was not disturbed by the diffusion of analytes and determined only by the infusion pressure. In addition, the study neglected the entrance effect at the end of the annulus since the length of the probe was approximately two orders of magnitude larger than the thickness of the annulus. Under these assumptions, the fluid velocity was only in the z-direction (v_z). The boundary conditions of v_z were $v_z = 0$ at $r = r_\alpha$ and at $r = r_\beta$, respectively. The analytical solution of the Navier–Stokes equation for v_z was:

$$v_z = \frac{2Q_d}{\pi r_\alpha^2} \frac{\ln(r/r_\alpha) - ((r/r_\alpha)^2 - 1)/(k^2 - 1)\ln(k)}{(k^2 + 1)\ln(k) + 1 - k^2} \quad (1)$$

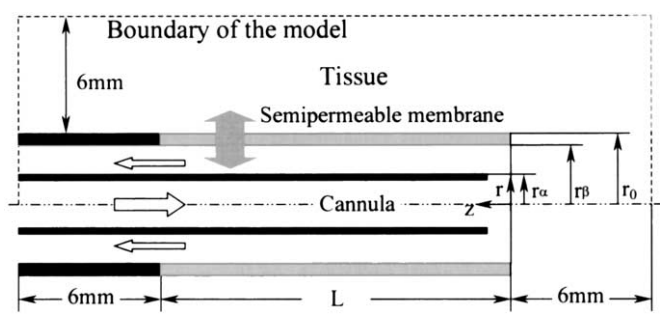

Fig. 1. Model geometry. The probe consisted of a hollow fiber with a cannula placed along the central axis. The membrane of the hollow fiber was permeable to analytes. The radii of the cannula, the inner membrane surface, and the outer membrane surface were r_α, r_β and r_0, respectively. The length of the probe, L, was defined as the length of the semipermeable membrane. The dashed line marked the region of simulations in the 2-D mathematical model, which was from 0 to $r_0 + 6$ mm in the r direction and from -6 mm to $L + 6$ mm in the z direction.

where Q_d was the perfusion rate in the probe, r_α was the radius of the outer surface of the inner cannula, r_β was the radius of the inner surface of the dialysate membrane, and k was the ratio of r_β/r_α. Transport of analytes in the probe involved convection in the z-direction and diffusion in both r- and z-directions:

$$v_z\frac{\partial C_d}{\partial z}=\frac{1}{r}\frac{\partial}{\partial r}\left(rD_d\frac{\partial C_d}{\partial r}\right)+\frac{\partial}{\partial z}\left(D_d\frac{\partial C_d}{\partial z}\right) \quad (2)$$

where C_d and D_d were the concentration and the diffusion coefficient of analytes in the dialysate, respectively.

2.1.3. Transport across the probe membrane

Diffusion was the dominant mode of transport across the probe membrane as discussed above. Diffusion in the semipermeable membrane was governed by the following equation:

$$0=\frac{1}{r}\frac{\partial}{\partial r}\left(rD_m\phi_m\frac{\partial C_m}{\partial r}\right)+\frac{\partial}{\partial z}\left(D_m\phi_m\frac{\partial C_m}{\partial z}\right) \quad (3)$$

where C_m and D_m are the concentration and the diffusion coefficient in the available space in the membrane, respectively, ϕ_m is the available volume fraction in the membrane.

2.1.4. Transport in the surrounding tissue

Microdialysis probe samples analytes that can be dissolved in the interstitial fluid. Transport of hydrophilic analytes through cells is in general negligible compared with that through the extracellular space. Therefore, transcellular transport was not considered in our model. The transport of analytes in the extracellular space involved interstitial convection, diffusion, and metabolism as well as transport across the microvessel wall. It has been well accepted that microdialysis will not induce convection in tissues. Thus, it was neglected in our model. The rate of metabolism of analytes was assumed to be proportional to the concentration. The rate of transport across the microvessel wall was assumed to be proportional to the concentration difference. The distribution of microvessels was assumed to be continuous and uniform throughout the tissue, since both the diameter of and the distance between microvessels are much smaller than the size of the region affected by microdialysis (Π). Taken together:

$$0=\frac{1}{r}\frac{\partial}{\partial r}\left(rD_e\phi_e\frac{\partial C_e}{\partial r}\right)+\frac{\partial}{\partial z}\left(D_e\phi_e\frac{\partial C_e}{\partial z}\right)-K_m\phi_eC_e+K_p\phi_e(C_p-C_e) \quad (4)$$

where C_e and D_e were the concentration and the diffusion coefficient in the interstitial fluid, respectively, ϕ_e was the available volume fraction of analytes in the extravascular space, K_m was the irreversible metabolism rate constant in the extravascular space, K_p was the exchange rate constant between the plasma and the interstitial fluid, and C_p was the concentration of analytes in the plasma.

2.1.5. Boundary conditions

The concentration of analytes outside the simulation region was nearly uniform. Thus, the concentration gradient was assumed to be zero at the surfaces of $z=-6$ mm, $z=6$ mm $+L$, and $r=6$ mm $+r_0$, respectively. Furthermore, we assumed that (i) $C_d=C_{in}$ at $z=0$ and $\partial C_d/\partial z=0$ at $z=6$ mm $+L$ in the annular region within the probe, (ii) the flux was zero on the surface of the inner cannula (i.e. $r=r_\alpha$), and (iii) the concentrations and the fluxes were continuous at the interfaces between dialysate and probe membrane as well as between probe membrane and surrounding tissues, respectively. The concentration of analytes in the interstitial fluid prior to microdialysis sampling (C_∞) was $C_pK_p/(K_m+K_p)$.

2.2. The equivalent length model

The BMD model predicts that:

$$E_d=1-\exp\left[-\frac{1}{Q_d(R_d+R_m+R_e)}\right] \quad (5)$$

where R_d, R_m and R_e were the transport resistances in the dialysate, probe membrane, and surrounding tissues, respectively. R_d and R_m can be estimated as:

$$R_d=\frac{13(r_\beta-r_\alpha)}{70\pi Lr_\beta D_d} \quad (6)$$

$$R_m=\frac{\ln(r_0/r_\beta)}{2\pi LD_m\phi_m} \quad (7)$$

To estimate R_e, the BMD model assumed that diffusion in tissues was only in the radial direction

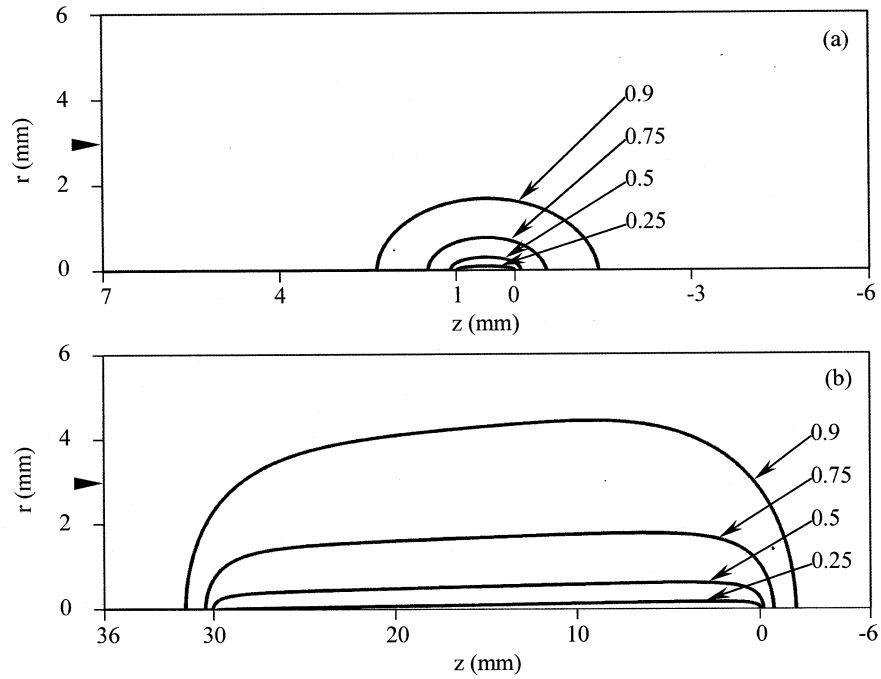

Fig. 2. Comparison of 2-D concentration distributions of sucrose in tissues surrounding (a) a short and (b) a long probe at the steady state. All model constants were fixed at the baseline values as shown in Table 1, except for the probe lengths being (a) 1 mm and (b) 30 mm, respectively. The perfusion rate was 1 μl/min in both cases. The concentration distributions in tissues were shown as iso-concentration lines. The concentration was normalized by C_∞.

and that transport in regions $z < 0$ and $z > L$ was negligible [10]. Based on this assumption, the mass balance equation predicts that:

$$R_e = \frac{\Gamma K_0(r_0/\Gamma)/K_1(r_0/\Gamma)}{2\pi r_0 L D_e \phi_e} \quad (8)$$

where K_0 and K_1 are the modified Bessel function of the second kind, of order zero and one, respectively, and Γ was the penetration depth defined as:

$$\Gamma = \sqrt{\frac{D_e}{(K_m + K_p)}} \quad (9)$$

We will show later that Eq. (8) overestimates R_e, since the 1-D assumption causes an underestimation of the total rate of analyte transport into the probe. The overestimation of R_e will in turn cause an underestimation of E_d (see Eq. (5)).

In order to correct the error without solving the 2-D model numerically, we developed an EL model of microdialysis sampling. The key idea in the new model was to construct a virtual probe whose length was longer than the actual one in order to compensate for the underestimation of E_d by the BMD model. As a result, Eqs. (5)–(8), could still be used to predict E_d, except that the length of the probe was replaced by an equivalent length (L_E) in Eq. (8). In general, LE depended on L and transport parameters of analytes in tissues. However, the quantitative relationship between these quantities could be complicated. Thus, we derived an approximate equation to estimate L_E. The derivation procedure is as follows.

A careful examination of 2-D concentration profiles shown in Fig. 2 suggested that the region affected by microdialysis sampling could be approximated by a cylinder with a hemisphere on either end. The length of the cylinder was the same as that of the probe. The radii of the cylinder and the two hemispheres were proportional to Γ. The proportionality constant was λ. As a first order approximation, we assumed that the con-

centrations were proportional to the radial distances in the cylinder and the hemispheres, respectively. Further, we assumed that the concentration of analytes at the border of the affected regions was C_∞ and the radius of the probe was negligible compared with $\lambda\Gamma$. When the metabolism was negligible compared with the transvascular transport, i.e. $K_m << K_p$, Eq. (4) predicted that $C_\infty \approx C_p$. Based on these assumptions, we found that the total rate of transport, J, from the tissue into the probe was:

$$J = \frac{1}{3}\pi C_\infty K_p \lambda^2 \Gamma^2 (L + \lambda\Gamma) \quad (10)$$

On the other hand, the total rate of transport could be derived based on the EL model, which assumed that the transport of analytes was 1-D within a cylinder with the length of L_E and the radius of $\lambda\Gamma$. Thus:

$$J = \frac{1}{3}\pi C_\infty K_p \lambda^2 \Gamma^2 L_E \quad (11)$$

Combination of Eqs. (10) and (11) gave:

$$L_E = L + \lambda\Gamma \quad (12)$$

The value of λ was determined through minimizing the differences in the predicted E_d between the 2-D and the EL models. The procedure of minimization is described in the next section.

Taken together, R_e in the EL model was estimated by:

$$R_e = \frac{\Gamma K_0(r_0/\Gamma)/K_1(r_0/\Gamma)}{2\pi r_0 (L + \lambda\Gamma) D_e \phi_e} \quad (13)$$

whereas R_d and R_m were still estimated by the same equations as those in the BMD model, i.e. Eqs. (6) and (7), respectively. Finally, the E_d in the EL model was calculated using Eq. (5).

2.3. Model constants and simulation procedures

2.3.1. Model constants

The baseline values of model constants are shown in Table 1. They were obtained from previous studies of microdialysis of sucrose in brain tissues [10]. In addition, we assumed that the rate of metabolism, K_m, was equal to zero in all simulations. The model constants were fixed at their baseline values in our simulations unless otherwise specified in figure legends. Variation in specific model constants was introduced in our simulations in order to determine effects of these constants on the error in the predicted E_d. The variation was based on the following considerations.

2.3.1.1. Diffusion coefficient. Microdialysis has been used to sample both small and large molecules. The difference in the size of molecules was reflected by the diffusion coefficient. In the present study, sucrose was used as an example of small molecules while dextrans with molecular weight (MW) of 20 000 (D20) and 50 000 (D50) were considered as examples of large molecules. The diffusion coefficients of D20 and D50 in water and granulation tissues in the rabbit ear chamber were calculated using the equations in [15]. For D20, $D_d = D_m = 1.11 \times 10^{-6}$ cm^2/s, $D_e = 1.86 \times 10^{-7}$ cm^2/s. For D50, $D_d = D_m = 7.15 \times 10^{-7}$ cm^2/s, $D_e = 1.23 \times 10^{-8}$ cm^2/s.

2.3.1.2. Exchange rate between the plasma and the interstitial fluid. The K_p of sucrose is tissue-dependent. It is equal to 2 per min in the liver [16] and 0.0021 per min in the brain. The range of K_p in other tissues is likely between these values. Thus, K_p was varied from 0.0021 to 2 per min.

Table 1
Baseline values of model constants[a]

Q_d (μl/min)	1
r_α (mm)	0.125
r_β (mm)	0.2
r_0 (mm)	0.25
L (mm)	3
D_d (cm^2/s)	7.0×10^{-6}
D_m (cm^2/s)	7.0×10^{-6}[b]
ϕ_m	0.2
D_e (cm^2/s)	3.1×10^{-6}
ϕ_e	0.175
K_m (per min)	0
K_p (per min)	2.1×10^{-3}

[a] All baseline values, except D_m, were obtained from [10].
[b] The diffusion coefficient of solutes in the membrane, D_m, was assumed to be equal to the diffusion coefficient in aqueous solution, D_d.

2.3.1.3. Available volume fractions. The ϕ_e is equal to 0.2 in the liver [17] and approximately 0.4 in a rat hepatoma (H5123) [18]. The baseline value of ϕ_m was 0.2. The situation with $\phi_m = 0.6$ was also simulated in the present study.

2.3.2. Procedures in numerical simulations

The 2-D model was solved numerically using a finite difference method described in [19]. For each set of model constants, Eq. (1) was first solved to obtain fluid velocity in the probe. The velocity profile was then substituted into Eq. (2), and Eqs. (2)–(4) were solved simultaneously to obtain concentration profiles and E_d through the line-by-line iteration method [19]. The program for numerical simulations was made by ourselves, based on VISUAL C^{++}. The probe length in the simulation varied from 1 to 30 mm. The simulated E_d was used to determine the value of λ in the EL model based on the least squares method in the KALEIDAGRAPH software. This value of λ was then substituted into the EL model to predict E_d when model constants other than the probe length were varied. The errors in predictions were calculated through comparing simulation results between EL/BMD and 2-D models. In all simulations, the error was calculated as a percentage of simulation results that deviated from those predicted by the 2-D model.

3. Results

We simulated 2-D concentration distributions at the steady state in tissues, based on the 2-D model described in Section 2. The iso-concentration lines are shown in Fig. 2. The arrow heads indicate the penetration depth, Γ. For both long and short probes, Γ was smaller than the size of our simulation region. To estimate the error caused by the assumption of 1-D diffusion in tissues, we calculated the relative difference in the predicted E_d between the BMD model and the 2-D model. We found that E_d could be well predicted by the BMD model when the probe was long (Fig. 3). The maximum error was $< 3\%$ for the 30-mm probe (Fig. 3). However, the error in

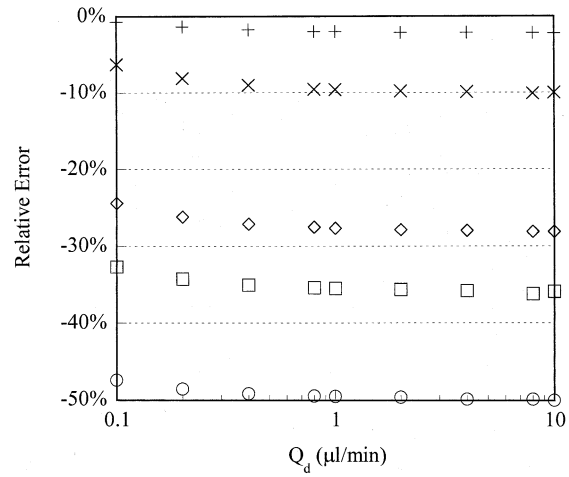

Fig. 3. The relative errors in E_d predicted by the BMD model. The predicted E_d was compared with that by the 2-D model for five different probes. The length of the probes were 1 mm (○), 2 mm (□), 3 mm (◇), 10 mm (×), and 30 mm (+), respectively. Other model constants were fixed at the baseline values as shown in Table 1. The relative errors were calculated as $(E_{d\_BMD} - E_{d\_2D})/E_{d\_2D}$.

BMD model predictions was increased when the probe length was decreased, and reached 50% when $L = 1$ mm (Fig. 3). In addition, we found that the error in BMD model predictions was not sensitive to the perfusion rate (Fig. 3), although E_d decreased exponentially as the perfusion rate was increased.

The error shown in Fig. 3 could be reduced if the EL model was used. The key parameter in the EL model was λ, which was determined numerically through minimizing the difference in the predicted E_d between 2-D and EL models. The difference was calculated for the set of model constants shown in Table 1, as well as for the variations in the probe length from 1 to 30 mm and the perfusion rate from 0.1 to 10 µl/min. The fitted value of λ was equal to 0.369. We then substituted the value of λ into the EL model and calculated the relative difference between EL and 2-D model predictions. The results are shown in Fig. 4. To further determine the accuracy of EL model predictions, relative errors in the predicted E_d based on other sets of model constants were calculated (Fig. 5). The maximum error found in all simulations was less than 6%.

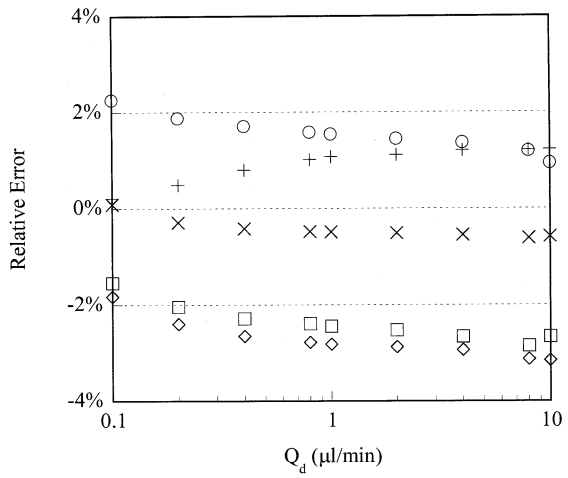

Fig. 4. The relative errors in curve-fitting of the EL model to the data of E_d generated by the 2-D model. The model constants, the meaning of symbols, and the error definition were identical to those in Fig. 3.

4. Discussion

An EL model was developed to minimize the error in the predicted E_d, based on the BMD model. The error analysis of both BMD and EL models covered the entire ranges of model constants found in microdialysis experiments. The analysis demonstrated that the BMD model was valid only for long probes. When the probe was short, the 1-D assumption in the BMD model caused a significant underestimation in E_d (Fig. 3), due to neglecting mass transfer into the probe from both regions of $z > L$ and $z < 0$. The error was reduced to less than 6% when the EL model was used (Figs. 4 and 5).

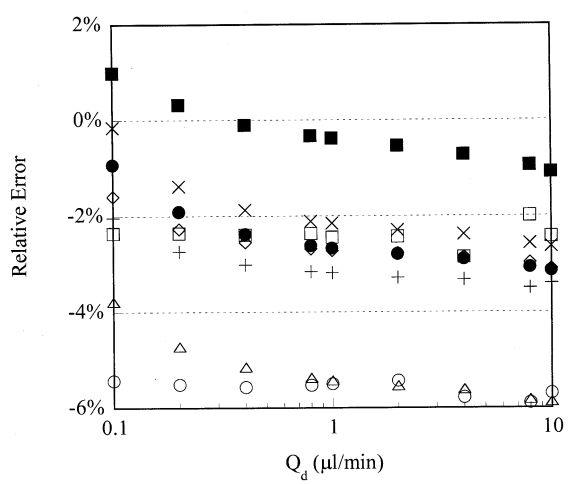

Fig. 5. Effects of model constants on the relative errors in E_d predicted by the EL model. λ was fixed at 0.369. The model constants were either fixed at the baseline values as shown in Table 1 or varied as follows: (○) $D_d = D_m = 1.11 \times 10^{-6}$ cm^2/s, $D_e = 1.86 \times 10^{-7}$ cm^2/s; (□) $D_d = D_m = 7.15 \times 10^{-7}$ cm^2/s, $D_e = 1.23 \times 10^{-8}$ cm^2/s; (◇) $\phi_e = 0.2$; (×), $\phi_e = 0.4$; (+), $\phi_m = 0.6$; (Δ), $K_p = 0.02$ per min; (●) $K_p = 0.2$ per min; (■) $K_p = 2$ per min.

There are at least two approaches to the correction of E_d predicted by the BMD model. One is to directly solve the 2-D model, using numerical methods. Another is to introduce an EL of probes in the calculation of tissue resistance to analyte transport. The second approach allowed investigators to use the same analytical equations as in the BMD model to predict E_d without solving differential equations numerically. Although EL model predictions are not 100% accurate, the maximum error was $< 6\%$ (Figs. 4 and 5). This range of error covers the case when the probe length approaches to the limit of cylindrical shape assumption, and is one order of magnitude smaller than that in BMD model predictions.

The perfusion rate had minimal effects on the error in the predicted E_d based on both BMD (Fig. 3) and EL (Fig. 4) models. However, it might significantly affect the concentration profiles shown in Fig. 2 and the value of E_d (data not shown). When the flow rate was extremely low (e.g. 0.1 μl/min) and the length of probe was very long (e.g. 30 mm), the concentration disturbance, caused by the perfusion in the probe, was limited only in a small volume near the tip of the probe. Beyond this region, concentration of analytes reached an equilibrium between the probe and surrounding tissues. On the other hand, the concentration equilibrium would never be reached when the perfusion rate was high and the probe was short. The effects of the perfusion rate on tissue concentration profiles, however, had minimal effects on the error in the predicted E_d shown in Figs. 3–5. The lack of effects was likely due to the fact that E_d depended on the total rate of transport rather than the details in concentration profiles of analytes in tissues.

Simulation results shown in Figs. 4 and 5 suggested that the error in the predicted E_d depended on all model constants. However, the maximum error in all cases was $<6\%$ (Figs. 4 and 5), although model constants had varied $\sim$2-fold for the available volume fraction (ϕ_e), $\sim$250-fold for the diffusion coefficient in tissues (D_e), and $\sim$950-fold for the rate of transvascular transport (K_p). These data suggested that the error in E_d predicted by the EL model was insensitive to model constants.

5. Conclusions

An EL model was developed in the present study. It allowed investigators to use simple and analytical equations (i.e. Eqs. (5)–(7) and (13)) to accurately predict E_d at the steady state for most microdialysis probes currently used in experiments. Thus, one does not have to numerically solve the 2-D transport equations unless the concentration profiles of analytes need to be calculated.

6. Nomenclature

E_d	extraction fraction
K_m	irreversible metabolism rate constant
K_p	exchange rate constant between the plasma and the interstitial fluid
L	probe length
L_E	equivalent length
Q_d	perfusion rate
r	radial distance from the probe axis
r_α, r_β, r_0	radial distance to outer surface of the inner cannula, inner surface and outer surface of dialysis membrane
v_z	flow velocity of dialysate in z direction
z	distance along probe axis
Π	the distance of concentration disturbance caused by microdialysis sampling
Γ	penetration depth in tissues
λ	$(L_E-L)/\Gamma$
k	r_β/r_α

Symbols with different subscripts

C	concentration of analytes
D	diffusion coefficient of analytes
R	transport resistance
ϕ	available volume fraction of analytes

Subscripts

d	dialysate
e	extracellular space in tissues
in	inlet
m	nembrane
out	outlet
p	plasma
∞	infinite

Acknowledgements

The work is supported in part by a grant from the National Institutes of Health (CA 87630).

References

[1] M. Muller, Adv. Drug Deliv. Rev. 45 (2000) 255–269.
[2] U. Ungerstedt, J. Intern. Med. 230 (1991) 365–373.
[3] T.E. Robinson, J.B. Justice, Microdialysis in the Neurosciences, Elsevier, Amsterdam, 1991.
[4] W.F. Elmquist, R.J. Sawchuk, Pharm. Res. 14 (1997) 267–288.
[5] M.I. Davies, Anal. Chim. Acta 379 (1999) 227–249.
[6] J.A. Stenken, Anal. Chim. Acta 379 (1999) 337–358.
[7] P. Rada, G.P. Mark, M.P. Vitek, R.M. Mangano, A.J. Blume, B. Beer, B.G. Hoebel, Brain Res. 550 (1991) 287–290.
[8] M.N. Woodroofe, G.S. Sarna, M. Wadhwa, G.M. Hayes, A.J. Loughlin, A. Tinker, M.L. Cuzner, J. Neuroimmunol. 33 (1991) 227–236.
[9] R. Landgraf, I. Neumann, F. Holsboer, Q.J. Pittman, Eur. J. Neurosci. 7 (1995) 592–598.
[10] P.M. Bungay, P.F. Morrison, R.L. Dedrick, Life Sci. 46 (1990) 105–119.
[11] J. Kehr, J. Neurosci. Methods 48 (1993) 251–261.
[12] H. Benveniste, A.J. Hansen, N.S. Ottosen, J. Neurochem. 52 (1989) 1741–1750.
[13] G. Amberg, N. Lindefors, J. Pharmacol. Methods 22 (1989) 157–183.
[14] P.F. Morrison, P.M. Bungay, J.K. Hsiao, B.A. Ball, I.N. Mefford, R.L. Dedrick, J Neurochem. 57 (1991) 103–119.
[15] R.K. Jain, Cancer Res. 47 (1987) 3039–3051.
[16] M. Ichikawa, S.C. Tsao, T.H. Lin, S. Miyauchi, Y. Sawada, T. Iga, M. Hanano, Y. Sugiyama, J. Hepatol. 16 (1992) 38–49.
[17] I.M. Arias, W.B. Jakoby, H. Popper, D. Schachter, The Liver Biology and Pathobiology, second ed., Raven, New York, 1988.
[18] P.M. Gullino, F.H. Grantham, S.H. Smith, Cancer Res. 25 (1965) 727–731.
[19] S.V. Patankar, Numerical Heat Transfer and Fluid Flow, McGraw-Hill, New York, 1980.